Title

DNA Rereplication Is Susceptible to Nucleotide-Level Mutagenesis

Journal

Genetics, 212(2)

ISSN

0016-6731

Authors

Bui, Duyen T

Li, Joachim J

Publication Date

2019-06-01

DOI

10.1534/genetics.119.302194

Peer reviewed

DNA Rereplication Is Susceptible to Nucleotide-Level Mutagenesis

Duyen T. Bui and Joachim J. Li[1]
Department of Microbiology and Immunology, University of California San Francisco, California 94143
ORCID IDs: 0000-0003-4231-0587 (D.T.B.); 0000-0002-5302-8897 (J.J.L.)

ABSTRACT The sources of genome instability, a hallmark of cancer, remain incompletely understood. One potential source is DNA rereplication, which arises when the mechanisms that prevent the reinitiation of replication origins within a single cell cycle are compromised. Using the budding yeast *Saccharomyces cerevisiae*, we previously showed that DNA rereplication is extremely potent at inducing gross chromosomal alterations and that this arises in part because of the susceptibility of rereplication forks to break. Here, we examine the ability of DNA rereplication to induce nucleotide-level mutations. During normal replication these mutations are restricted by three overlapping error-avoidance mechanisms: the nucleotide selectivity of replicative polymerases, their proofreading activity, and mismatch repair. Using *lys2InsE*$_{A14}$, a frameshift reporter that is poorly proofread, we show that rereplication induces up to a 30× higher rate of frameshift mutations and that this mutagenesis is due to passage of the rereplication fork, not secondary to rereplication fork breakage. Rereplication can also induce comparable rates of frameshift and base-substitution mutations in a more general mutagenesis reporter *CAN1*, when the proofreading activity of DNA polymerase ε is inactivated. Finally, we show that the rereplication-induced mutagenesis of both *lys2InsE*$_{A14}$ and *CAN1* disappears in the absence of mismatch repair. These results suggest that mismatch repair is attenuated during rereplication, although at most sequences DNA polymerase proofreading provides enough error correction to mitigate the mutagenic consequences. Thus, rereplication can facilitate nucleotide-level mutagenesis in addition to inducing gross chromosomal alterations, broadening its potential role in genome instability.

KEYWORDS DNA replication fidelity; rereplication; mismatch repair; genome instability; DNA polymerase proofreading

To ensure that every chromosomal segment is replicated once and only once, eukaryotic cells initiate DNA replication at thousands of replication origins scattered throughout their genome and employ multiple overlapping mechanisms to prevent reinitiation at these origins (Nguyen *et al.* 2001; Truong and Wu 2011; Abbas *et al.* 2013; Siddiqui *et al.* 2013). These mechanisms are regulated during the cell cycle and inhibit proteins required for the initiation of DNA replication after they have executed key initiation functions. In G1 phase, the Origin Recognition Complex (ORC), Cdc6, Cdt1, and the Mcm2-7 core replicative helicase license origins for initiation in S phase by loading the ring-shaped Mcm2-7 helicase around origin DNA. Subsequently, during the exit from G1 phase, the licensing activities of these proteins are downregulated in a multitude of ways to prevent relicensing and reinitiation for the remainder of the cell cycle.

These inhibitory mechanisms cooperate in a multiplicative fashion to minimize the probability that any origin reinitiates within the genome. When only a single mechanism is disrupted, the increase in reinitiation frequency is apparently too low to result in enough rereplication to be detected by current assays. However, as more and more mechanisms are disrupted, reinitiation and rereplication become detectable, and progressively larger in amount (Nguyen *et al.* 2001; Green *et al.* 2010). Understanding the consequences of disrupting reinitiation controls may be of relevance to cancer, as the deregulation of replication initiation proteins has both been observed in cancers (Karakaidos *et al.* 2004; Tatsumi *et al.* 2006; Liontos *et al.* 2007) and shown to potentiate oncogenesis in animal models (Arentson *et al.* 2002; Seo *et al.* 2005; Liontos *et al.* 2007).

doi: https://doi.org/10.1534/genetics.119.302194
Manuscript received December 21, 2018; accepted for publication April 15, 2019; published Early Online April 26, 2019.
Available freely online through the author-supported open access option.
Supplemental material available at FigShare: https://doi.org/10.25386/genetics.8046347.
[1]Corresponding author: Department of Microbiology and Immunology, Box 2200, 600 16th St., University of California San Francisco, San Francisco, CA 94143. E-mail: Joachim.Li@ucsf.edu

We have previously established in the budding yeast *Saccharomyces cerevisiae* that rereplication arising from disruptions in reinitiation control can be an extremely potent source of gross chromosomal alterations, specifically intrachromosomal gene amplification (Green *et al.* 2010) and whole-chromosome aneuploidy (Hanlon and Li 2015). These gross chromosomal alterations are stimulated in part because rereplication forks are highly susceptible to breakage (Finn and Li 2013; Alexander and Orr-Weaver 2016), which in turn triggers recombinational repair pathways that can generate rearrangements (Finn and Li 2013). Although the basis for the rereplication fork breakage that we see is not clear, the compromised integrity of these forks suggests they might differ in fundamental ways from S-phase replication forks. This prompted us to ask whether the fidelity of DNA replication might also be compromised during rereplication.

Three mechanisms ensure the fidelity of normal S-phase replication [reviewed in Kunkel (2009) and Ganai and Johansson (2016)]: (1) the nucleotide selectivity of the polymerase activity of the replicative DNA polymerases, polymerase ε (Pol ε) and polymerase δ (Pol δ); (2) the proofreading excision of misincorporated and/or mismatched primer nucleotides by the 3′ to 5′ exonuclease activity of Pol ε and Pol δ; and (3) a postreplicative mismatch repair (MMR) system that cooperates with DNA replication to detect, excise, and replace any remaining mismatched nucleotides on newly replicated daughter strands. These mechanisms work in series and cooperate in a multiplicative manner (Morrison *et al.* 1993; Tran *et al.* 1999; Greene and Jinks-Robertson 2001; Lujan *et al.* 2012; Buckland *et al.* 2014; St Charles *et al.* 2015; Schmidt *et al.* 2017) to reduce the rate of nucleotide-level errors (*e.g.*, base substitutions and small insertions/deletions) to $\sim 10^{-10}$ per replicated nucleotide. They also appear to operate with some redundancy, because the loss of fidelity due to partial disruption of an error-avoidance mechanism is often not fully manifested until another mechanism is disrupted (Tran *et al.* 1999; Deem *et al.* 2011; St Charles *et al.* 2015; Schmidt *et al.* 2017).

When replication forks are stalled or stressed by local impediments, such as DNA damage or short-hairpin structures, these mechanisms may be circumvented by the transient substitution of error-prone polymerases for replicative polymerases as the cell tries to bypass the problem (Northam *et al.* 2014; Makarova and Burgers 2015; Vaisman and Woodgate 2017). Not only do these polymerases have lower nucleotide selectivity and lack proofreading function, the errors introduced by DNA polymerase ζ (Pol ζ), the error-prone polymerase required for much of the mutagenesis in budding yeast, do not seem to be edited by MMR (Huang *et al.* 2002; Lehner and Jinks-Robertson 2009; Aksenova *et al.* 2010; Kochenova *et al.* 2015).

In this study, we show that the fidelity of DNA rereplication is reduced > 30-fold relative to replication as assayed by reversion of *lys2InsE*$_{A14}$, a sensitized frameshift reporter that is poorly proofread (Tran *et al.* 1997). We provide evidence that the mutagenesis is caused by rereplication *per se* and not by break repair-induced mutagenesis arising from nearby rereplication fork breakage. At a more general mutagenesis reporter, *CAN1*, the compromised fidelity of rereplication is partially masked by the redundancy of fidelity mechanisms but can be uncovered by inactivating the exonuclease proofreading activity of Pol ε. This rereplication-induced *lys2-InsE*$_{A14}$ reversion and *CAN1* mutagenesis is not dependent on Pol ζ, suggesting that rereplication is not increasing error rates by promoting more frequent bypass of the canonical error-avoidance mechanisms. Instead, we find that the higher mutagenesis of rereplication *vs.* replication is lost in MMR null strains, suggesting that rereplication compromises nucleotide fidelity by attenuating MMR. Thus, in addition to inducing extremely high levels of gross chromosomal rearrangements, rereplication can facilitate nucleotide-level mutagenesis.

Materials and Methods

Nucleotide and chromosomal positions

Nucleotide positions in the chromosomes are reported based on the S288c reference sequence in the *Saccharomyces* Genome Database (R64.2.1, 2014-11-18) (Engel *et al.* 2014). Nucleotide positions of deleted gene segments are reported relative to the A of the start codon, with positive numbers 3′ of the A (+1) and negative numbers 5′. Chromosomal positions of mutagenesis reporter genes are reported to the nearest kilobase (kb) of their insertion site. *URA3* fragments were inserted at the boundaries of the amplified segment in place of clusters of repetitive sequences elements (Ty elements and adjacent tRNA genes, and long terminal repeats) (Finn and Li 2013); the insertion sites of these fragments are reported as the positions at the edges of the amplified segment.

Oligonucleotides

Oligonucleotides used as PCR or sequencing primers in plasmid constructions, strain constructions, and mutational analyses are listed in Supplemental Material, Table S1.

Plasmids

All plasmids used in this study are listed in Table S2. pDB101 contains a *LYS2-CAN1* cassette and was used as the PCR template for generating cassette fragments that were integrated at various positions in chromosome IV. The cassette was generated by two rounds of PCR. In the first round, the *LYS2* (−450 to +4524) and *CAN1* (−829 to +2515) genes were separately amplified by PCR from S288c genomic DNA with primer tails that generate 40 bp of overlap between the two fragments. In the second round, these fragments were then used as templates for fusion PCR to generate a *Sac*I-*LYS2-CAN1-Xma*I fragment containing both genes in the same orientation with *LYS2* upstream of *CAN1*. This fragment was cloned into the *Sac*I and *Xma*I sites of pRS306 (Sikorski and Hieter 1989) to form pDB101.

pDB107 is derived from a clustered regularly interspaced short palindromic repeats (CRISPR)-Cas9 targeting vector (pRS425-CAS9-2XSapI) developed in Bruce Futcher's

laboratory (Zhao *et al.* 2016). pRS425-CAS9-2XSapI constitutively expresses Cas9 from the *TEF1* promoter and a CRISPR single-guide RNA (sgRNA) from the *SNR52* promoter. Two closely spaced *Sap*I sites in a nonspecific 20-bp targeting sequence at the beginning of the sgRNA allow replacement of the nonspecific sequence with a desired 20-bp targeting sequence. pRS425-CAS9-2XSapI also contains a *LEU2* marker, and a 2 micron replication origin and stability locus. In pDB107 two changes were made: (1) complementary oligonucleotides OJL4249 and OJL4250 were cloned between the two *Sap*I restriction sites to target *POL2* for CRISPR-Cas9 cleavage and mutation to *pol2-4*, and (2) the *LEU2* marker was replaced by hphMX from pRS40H (Chee and Haase 2012). pDB114 was constructed from pDB107 by replacing the 2 micron elements with the *CEN6-ARS209* cassette from pRS414 (Sikorski and Hieter 1989).

Strains

Yeast strains used in this study were descendants of YJL8363 and YJL9149 (Green *et al.* 2010; Finn and Li 2013), and are listed in Table S3. The YJL8363 genotype deregulates three replication initiation proteins that are normally inhibited by Clb cyclin-dependent kinase (CDK) to prevent the reinitiation of DNA replication: (1) *MCM7-2NLS* confers constitutive nuclear localization on the Mcm2-7 core replicative helicase (Nguyen *et al.* 2000); (2) *ORC6-cdk1A(S116A)* disrupts one of four consensus CDK phosphorylation sites on Orc6 (Nguyen *et al.* 2001); and (3) *pGAL-ΔntCDC6-cdk2A* provides galactose-inducible overexpression of stabilized ΔntCDC6-cdk2A on top of the normal cell cycle-regulated expression of Cdc6 from the wild-type *CDC6* gene (Nguyen *et al.* 2001; Perkins *et al.* 2001). Exposing cells to galactose induces detectable reinitiation most prominently from one origin, *ARS317* (Green *et al.* 2006; Richardson and Li 2014). In YJL8363, this origin has been removed from its endogenous location on chromosome III and inserted into chromosome IV (Figure 1A). YJL8363 also contains a split *URA3* reporter for rereplication-induced gene amplification (RRIGA) of a 124-kb segment of chromosome IV spanning the inserted *ARS317*. The 3′ (*RA3*) and 5′ (*UR*) portions of this split reporter replace the Ty retrotransposons that originally formed the boundaries of this amplified segment in the predecessor strain for YJL8363 (Green *et al.* 2010; Finn and Li 2013). Intrachromosomal amplification via nonallelic homologous recombination between the 390 bp of overlapping sequence identity in *RA3* and *UR* reconstitutes an intact *URA3* reporter at the junction between adjacent tandem amplified segments (Finn and Li 2013). YJL9149, the nonrereplicating control strain, is congenic with YJL8363, but has *pGAL* in place of *pGAL-ΔntCDC6-cdk2A*.

YJL11037 and YJL11035 were derived from YJL8363 and YJL9149, respectively, by introducing precise deletions of both *LYS2* (*lys2*Δ) and *CAN1* (*can1*Δ) open reading frames (ORFs) into the latter two strains. The *lys2*Δ and *can1*Δ deletion fragments were both generated by two successive rounds of PCR: the first round synthesized a primer dimer with 40 bp homology to the sequences just outside both ends of the deleted ORF; the second round extended the homology to 70 bp using the primer dimer as template. *lys2*Δ isolates were obtained by transforming cells with the *lys2*Δ deletion fragment and selecting for survivors on α-aminoadipic acid plates (Chattoo *et al.* 1979). *can1*Δ isolates were obtained by transforming cells with the *can1*Δ deletion fragment and selecting for survivors on canavanine plates. Chromosomal deletions were confirmed by PCR of the expected size fragments spanning the deletions.

The *LYS2-CAN1* cassette from pDB101 was integrated into the rereplicating strain YJL11037 at one of four locations on chromosome IV to form YJL11071 (ChrIV_570 kb), YJL11073 (ChrIV_637 kb), YJL11075 (ChrIV_795 kb), and YJL11077 (ChrIV_1081 kb). The cassette was also integrated into the nonrereplicating strain YJL11035 at the same positions to form YJL11049 (ChrIV_570 kb), YJL11066 (ChrIV_637 kb), YJL11067 (ChrIV_795 kb), and YJL11069 (ChrIV_1081 kb). Integrating fragments containing 60 bp of homology flanking the integration sites were generated by two successive rounds of PCR from pDB101. After selecting for Lys^+ yeast transformants, integration at the correct sites was confirmed by PCR across the integration junctions on both sides of the cassette. The sequence of the integrated *CAN1* was confirmed by PCR amplification and sequencing.

The *lys2InsE*$_{A14}$ and *lys2InsE*$_{A10}$ reporters were substituted for *LYS2* in strains containing the *LYS2-CAN1* cassettes. Fragments containing almost the entire *lys2InsE*$_{A14}$ and *lys2InsE*$_{A10}$ reporters were excised (with *Nru*I and *Hin*dIII), respectively, from plasmids p233 and p10A-2-Int1, which were obtained from the Gordenin/Resnick laboratories (Tran *et al.* 1997). Strains transformed by these fragments were plated on α-aminoadipic acid plates (Chattoo *et al.* 1979) to select for integration of the reporters, and successful replacement of the *LYS2* sequence was confirmed by PCR with OJL4084 and OJL4218 to check for the presence of the *InsE* insert.

The *pol2-4* mutation (Morrison *et al.* 1991) was introduced into *lys2InsE*$_{A14}$*-CAN1* reporter strains by CRISPR-Cas9 editing. The edited strains were the rereplicating strains YJL11108 (ChrIV_570 kb reporters) and YJL11112 (ChrIV_637 kb reporters), and the nonrereplicating strains YJL11130 (ChrIV_570 kb reporters) and YJL11090 (ChrIV_637 kb reporters). These strains were cotransformed with a CRISPR-Cas9 plasmid targeting *POL2* (either pDB107 or pDB114) and a *pol2-4* donor template generated by two rounds of PCR. In the first round of PCR, genomic DNA from S288c was used as template to PCR two overlapping segments from *POL2* with the *pol2-4* mutation (D290A and E292A) and a silent mutation (V286V) in the overlap region. The silent mutation disrupts the sequence targeted by the CRISPR-Cas9 plasmid, so once Cas9-cleaved *POL2* is repaired with the *pol2-4* donor template, the resulting *pol2-4* allele is protected from further cleavage. In the second round, the

two overlapping segments were used as templates for fusion PCR. Surviving yeast isolates from the CRISPR-Cas9 transformation were screened for the presence of the *pol2-4* mutation by PCR amplification and sequencing, using primers OJL4255 and OJL4258.

YJL11234–YJL11236 were generated from YJL11108 (*lys2InsE$_{A14}$-CAN1* reporter inserted in ChrIV_570 kb) by introducing a deletion of the *MSH2* ORF marked by *TRP1*. A *msh2*Δ::*TRP1* deletion fragment was generated by two successive rounds of PCR: in the first round, pRS414 (Sikorski and Hieter 1989) was used as a template to PCR a *TRP1* fragment flanked by 30 bp of homology to sequences just outside the *MSH2* ORF; in the second round, this fragment was used as a template to extend the flanking homology to 60 bp. After selecting for Trp$^+$ transformants, we screened for the *msh2*Δ::*TRP1* deletion by PCR across the junctions on both sides of the deletion.

Strain growth and media

For standard growth, yeast were grown on rich yeast extract, peptone media (YPD) or synthetic complete media (SDC) containing 2% w/v dextrose (D16; Fisher Scientific, Pittsburgh, PA) as previously described (Green *et al.* 2010). Before the induction of rereplication with 2.7% w/v galactose (G0750; Sigma [Sigma Chemical], St. Louis, MO), cells were grown overnight in YPRd, rich yeast extract peptone media containing 3% w/v raffinose (R1030; US Biological) and 0.1% w/v dextrose, or in a few experiments for 3 hr in YPR, rich media containing 3% w/v raffinose. These media allow gradual release from dextrose-mediated repression of the *pGAL* promoter, so that the promoter can be rapidly induced upon the addition of galactose (Johnston 1987). To quantify Lys$^+$ revertants, cells were plated on SDC-LYS. To quantify canavanine-resistant mutants, cells were plated on canavanine plates [SDC-ARG plates containing 60 μg/ml canavanine (C9758; Sigma)]. To quantify cells that had undergone segmental amplification and reconstituted the *URA3* amplification reporter at the amplification junction, cells were plated on SDC-URA. To determine the total number of colony forming units in experimental cultures, cells were plated on SDC.

Measuring basal and rereplication-induced mutation rates

Basal mutation rates were determined by measuring the rate of mutant accumulation during the expansion of yeast cultures from single cells (Drake 1991). Rereplication-induced mutations rates were determined by measuring the increase in mutants after 3 hr of rereplication in nocodazole-arrested cells.

Specifically, yeast strains were struck for single colonies from frozen yeast stocks onto YPD plates and grown at 30°. For most strains, an entire colony grown from a single cell for 30 hr was transferred into 50–100 ml of liquid YPRd, and grown for an additional 13–16 hr at 30° until the culture reached an OD_{600} between 0.2 and 0.5 (~0.4–1.0 × 10^7 cells/ml). At that point, 10 mg/ml nocodazole (N3000; US Biological) in DMSO (ICN19481950; Fisher Scientific) was added to the culture to a final concentration of 15 μg/ml. After 2.5 hr incubation, mitotic arrest was confirmed microscopically (> 90% large-budded cells), and 40% galactose was added to a final concentration of 2.7% w/v to induce rereplication. At $T = 0$ and $T = 3$ hr of galactose induction, cells were plated on SDC plus one or more of the following plates: SDC-LYS, SDC-URA, and canavanine. Cells were concentrated or diluted before plating such that most plates yielded 50–250 colonies. These were counted after 2–3 days of incubation at 30°.

From the $T = 0$-hr plating on SDC we obtained N, the total number of cells that grew out from a single cell. From the $T = 0$-hr plating on SDC-LYS, SDC-URA, and canavanine (and the value of N) we obtained f_0, the fraction of mutant cells that had accumulated in the culture with Lys$^+$, Ura$^+$, and Can^R phenotypes, respectively. N and f_0 were then used to solve u, the basal mutation rate, in Drake's formula $\mu = f/\ln(\mu N)$ (Drake 1991). Similarly, from the $T = 3$-hr plating we obtained f_3, the fraction of mutant cells present after the induction of rereplication for each of the mutant phenotypes that were plated (Lys$^+$, Ura$^+$, or Can^R). For each phenotype, the difference $f_3 - f_0$ yielded the rereplication-induced mutation rate. For each genotype, experiments were performed with 3–25 biological replicas using at least two congenic sister isolates. For each pair of basal and induced rates, we report the mean rate and SEM, and perform statistical comparison between the two rates using the Mann–Whitney *U*-test (Mann and Whitney 1947). For the results described in Table S11, we used the Mann–Whitey *U*-test to compare the ratios of (induced rate of Lys$^+$ Ura+) /(induced rate of Ura$^+$) for two different genotypes. The Mann–Whitney Test Calculator from Social Science Statistics was used to calculate the *P*-value for significance (https://www.socscistatistics.com/tests/mannwhitney/default2.aspx). Throughout the manuscript we have used a significance level of 0.01.

Several experiments involving the *msh2*Δ strains YJL11234–YJL11236 used a modified outgrowth and induction protocol. Because of their high basal mutation rate, in some experiments these strains were grown for fewer generations during the mutation accumulation period. Colonies grown from single cells for 35–42 hr on YEPD plates were transferred to 50 ml of liquid YPR and incubated for only 3 hr till they reached an OD_{600} of only 0.01–0.10 before the addition of nocodazole. After arrested cells were plated for the $T = 0$-hr time point, the remaining culture was split into two. Galactose was added to one culture (final concentration 2.7% w/v) to induce rereplication and dextrose was added to the other (final concentration 2.7% w/v) as a negative rereplication control.

Finally, in some experiments, we wished to measure the rereplication-induced reversion rate for the subpopulation of *lys2InsE$_{A14}$* reporters that had experienced a rereplication-induced gene amplification. In principle, one could first select for the latter population by plating on SDC-URA, then replica

plate to SDC-URA, LYS to quantify the fraction of amplified reporters that had also reverted to Lys^+ when they rereplicated. However, during the outgrowth of colonies on SDC-URA plates, Lys^+ revertants would be generated independently of rereplication, preventing us from accurately scoring just those colonies that became Lys^+ due to rereplication. Hence, we instead performed virtual replica plating by simultaneously plating cells on SDC, SDC-URA, and SDC-URA, LYS at both $T = 0$ and $T = 3$ hr, then dividing the fraction of total cells that became Ura^+ Lys^+ after rereplication by the fraction of total cells that became Ura^+ after rereplication. Both fractions were calculated from the $f_3 - f_0$ difference for their respective phenotypes.

Monitoring rereplication via array comparative genomic hybridization

For those experiments in which rereplication was monitored by array comparative genomic hybridization (aCGH), $\sim 2 \times 10^8$ cells were harvested for genomic DNA preparation after the $T = 3$-hr plating described above. This rereplicating genomic DNA was prepared by method 1 as described in Finn and Li (2013). For aCGH reference DNA, nonreplicating genomic DNA from YJL8427 and YJL6977 were prepared by method 2 as described in Finn and Li (2013). Subsequent aCGH steps were performed essentially as described in Green *et al.* (2010). Briefly, 90% of the rereplicating DNA preparation and 1 μg of the reference DNA were labeled, respectively, with Cy3 and Cy5 fluorescent dye (45-001-270; Fisher Scientific). The Cy3- and Cy5-labeled DNAs were isolated, combined, and applied to microarrays printed in-house for hybridization at 65° for at least 18 hr. Arrays were then scanned using an Axon Scanner 4B. GenePix Pro 6.0 and BatchReplicationAnalyzer4.2 (Green *et al*. 2010) were then used to generate copy number information across the genome.

Data availability

Plasmids and strains are available upon request. Tables S1–S3 list oligonucleotides, plasmids, and strains used in this study. Tables S3–S11 and S13–S21 list the basal and induced amplification rates for the experiments described in this study. Table S12 lists mutations identified in various Can^R isolates. Figure S1 shows the rereplication profiles of strains used in Figure 2A. Figure S2 shows the amplification rates of the strains used in Figure 2A. Figure S3 shows the reversion rate for the *lys2InsE$_{A10}$* reporter. Figure S4 shows the amplification rates of the strains used in Figure 3. Figure S5 shows the mutation rates for *lys2InsE$_{A14}$* and *CAN1* in MMR mutant strains. Figure S6 shows the amplification rates of the strains used in Figure 6 and Figure S5. Figure S7 shows the amplification rate of the strains used in Figure 7. All raw and processed aCGH data have been deposited with the Gene Expression Omnibus (GEO) database and assigned accession number GSE124382. Supplemental material available at FigShare: https://doi.org/10.25386/genetics.8046347.

Results

DNA rereplication induces an elevated frameshift mutation rate

To determine whether rereplication induces increased rates of nucleotide-level mutations, we used our previously published *S. cerevisiae* system for conditionally inducing transient and localized rereplication (Green *et al.* 2010; Finn and Li 2013). In this system, we conditionally deregulate a subset of replication initiation proteins in metaphase-arrested cells by the addition of galactose to the media. Using aCGH to monitor the increase in copy number across the genome, we have previously shown that this deregulation induces a stereotypical rereplication profile with overt reinitiation occurring most prominently from one origin, *ARS317*, at position 567 kb on chromosome IV (Figure 1A). By 3 hr of induction, ~50% of the *ARS317* has reinitiated with rereplication forks proceeding bidirectionally away, but progressively dropping out with increasing distance from the origin. After induction, cells are released from the arrest in the presence of dextrose, which represses further rereplications. This protocol allows us to assess the genomic consequences of a transient, limited, and localized induction of rereplication within one cell cycle.

One of these consequences, amplification of a large 124-kb chromosomal segment spanning *ARS317*, can be detected with a split *URA3* reporter (Finn and Li 2013). In this system, a 3′ *RA3* segment and a 5′ *UR* segment, sharing 390 bp of overlapping sequence identity, are positioned at the boundaries of the amplified segment at 521 and 645 kb (Figure 1A). Rereplication induced gene amplification (RRIGA) of this segment reconstitutes *URA3* at the interamplicon junction, allowing for selection of these recombination events. Seeing a strong persistent induction of RRIGA in the experiments described below provides some assurance that the degree of rereplication, the extent of rereplication fork progression and breakage, and the recombinational repair of these breaks is not significantly affected in most of these experiments.

To measure the rate of mutagenesis during rereplication, we inserted a cassette containing two reporter genes at one of four positions in the path of rereplication forks originating from *ARS317*. As expected, these insertions—at 3, 68, 228, and 514 kb to the right of *ARS317* (Figure 1A)—did not alter the rereplication profiles of these strains (Figure S1). One of these reporters, *lys2InsE$_{A14}$*, has previously been used as a sensitized detector of frameshift mutagenesis (Tran *et al.* 1997). It contains a small insertion with an A14 homopolymeric tract that inactivates the *LYS2* gene by introducing a frameshift (Figure 1B). DNA polymerases replicating through the A14 tract are susceptible to replication slippage, which can introduce compensatory frameshift mutations that generate selectable Lys^+ revertants. The other reporter, *CAN1*, detects more generic frameshifts or base substitutions (Huang *et al.* 2002; Lang and Murray 2008), which inactivate the gene and confer resistance to the toxic arginine analog canavanine (Figure 1C).

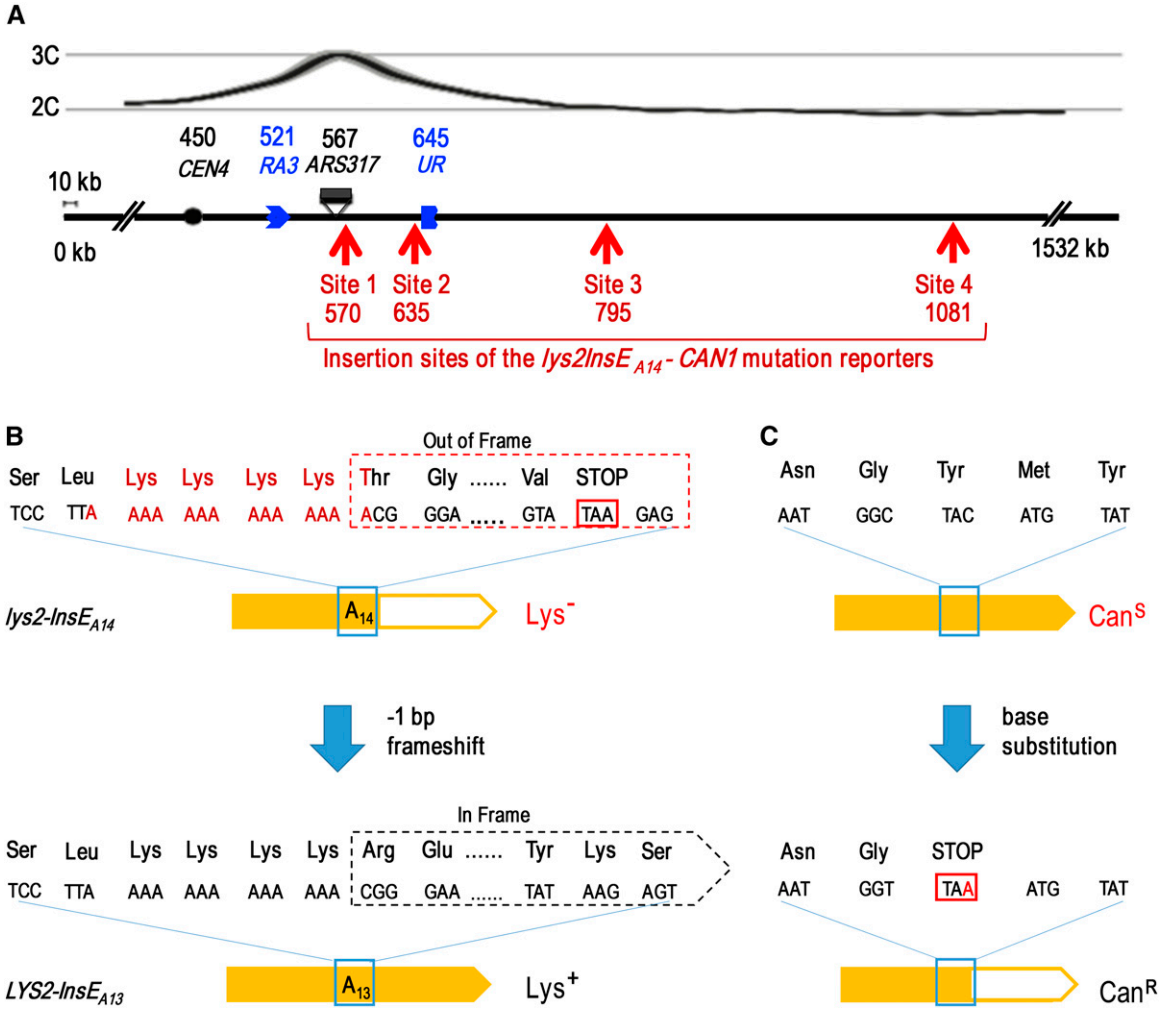

Figure 1 System for inducing localized rereplication and measuring mutation frequency. (A) Schematic of chromosome IV showing the chromosomal positions in kilobases (kb) of *CEN4*, the inducible reinitiating origin *ARS317*, the segmental duplication reporters (3′ *RA3* and 5′ *UR* overlapping fragments of *URA3*), and insertion sites (red arrows) for the mutation reporter cassettes (*lys2InsE*$_{A14}$ - *CAN1*). Rereplication-induced segmental duplication occurs via nonallelic homologous recombination between the 390-bp overlap sequence shared by the *RA3* and *UR* fragments (see Figure 4A), and reconstitutes *URA3* at the boundary between the duplicated segments (Finn and Li 2013). Shown above is the typical rereplication copy number profile of chromosome IV after reinitiation has been induced for 3 hr during a nocodazole arrest [reproduced from Finn and Li (2013)]. The decline in copy number at increasing distance from *ARS317* is due to the decreasing number of rereplication forks that can travel these distances from *ARS317*. (B) The *lys2InsE*$_{A14}$ reporter (Tran *et al.* 1997) contains a homopolymeric run of 14 As, which introduces an inactivating frameshift in the *LYS2* coding sequence. Compensatory frameshift mutations that restore the correct frame confer a dominant selectable Lys$^+$ phenotype. (C) The *CAN1* gene, which encodes the high-affinity arginine permease, makes cells sensitive (Can^S) to the toxic arginine analog canavanine. Inactivating frameshift or base substitution mutations (such as the nonsense mutation shown) confer a recessive selectable canavanine resistance (Can^R) phenotype.

Figure 2A shows how we measured the baseline and rereplication-induced mutation rates of these reporters. Cell cultures derived from single cells were arrested in metaphase with nocodazole, then galactose was added for 3 hr to transiently induce rereplication. Just before ($T = 0$ hr) and after ($T = 3$ hr) this induction, cells were plated to quantify the frequency of Lys$^+$ and Can^R mutants. To determine the baseline mutation rate of these reporter genes during the expansion of the culture from a single cell, we applied Drakes' formula for mutation accumulation (Drake 1991) to the mutant frequency at $T = 0$ hr. To determine the rereplication-induced mutation rate we took the difference in mutant frequency at $T = 3$ and $T = 0$ hr.

The baseline mutation rates at the four insertion sites on chromosome IV for the *lys2InsE*$_{A14}$ reporter were similar (3–6 $\times$ 10^{-7}) (Figure 2B and Table S4) and within the range observed in previous reports (Tran *et al.* 1997; Deem *et al.* 2011; Bui *et al.* 2015). After transient induction of rereplication, the *lys2InsE*$_{A14}$ reporter at site 1 (within 3 kb from *ARS317*) experienced a 15-fold increase in reversion rate above its basal rate (Figure 2B and Table S4). At this position ~50% of chromosome IV is rereplicated (Figure 1A), making the normalized reversion rate for a fully rereplicated *lys2InsE*$_{A14}$ reporter ~30-fold above basal rates. At site 2 (68-kb away from *ARS317*), where ~25% of chromosome IV is rereplicated (Figure 1A), the induced reversion rate was

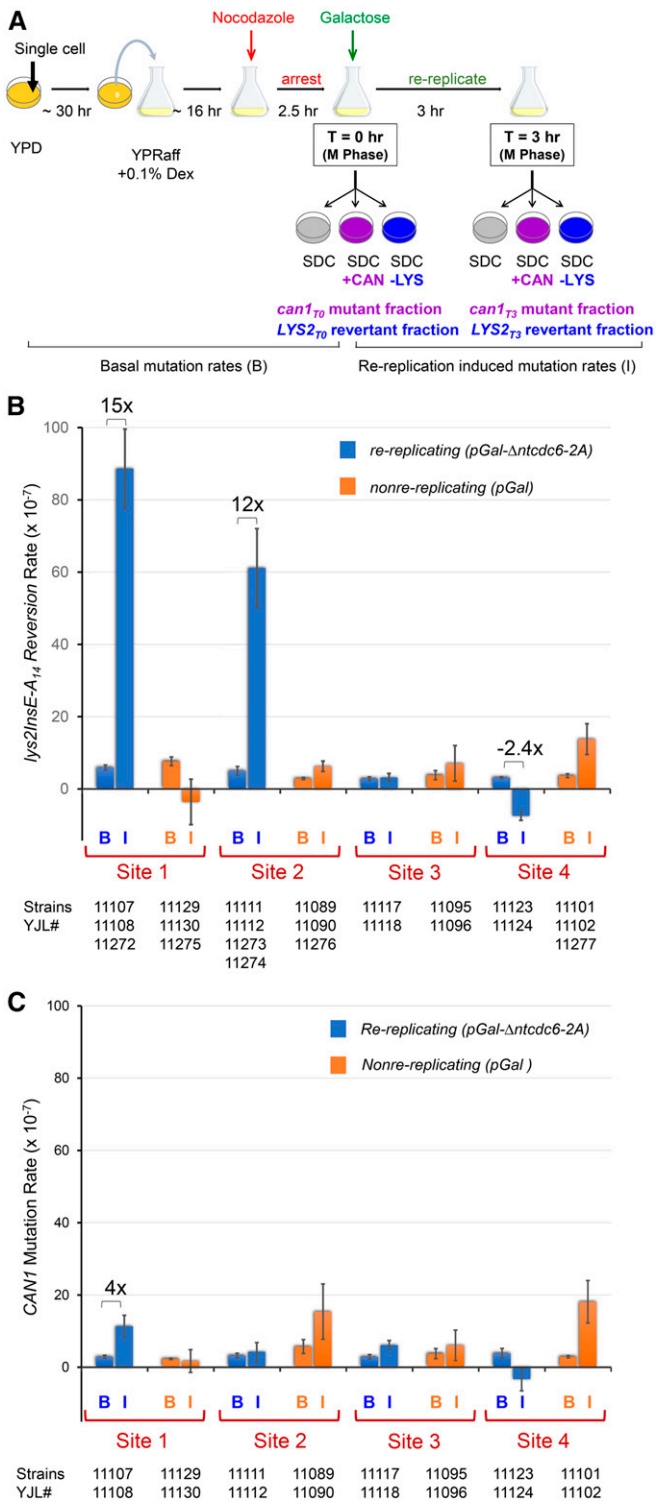

Figure 2 Rereplication increases the reversion rate of the *lys2InsE$_{A14}$* reporter. (A) Assay for quantifying basal and rereplication-induced mutation rates. Galactose-inducible rereplicating strains (*orc6-cdk1A MCM7-2NLS pGAL-Δntcdc6-2A*, see text) were grown from single cells under non-inducing conditions then arrested in metaphase by the addition of nocodazole. At *T* = 0 hr, cells were plated to quantify the frequency of Lys$^+$ or Can^R mutants that had accumulated during this outgrowth, and basal mutation rates were calculated from this frequency using Drake's formula (Drake 1991). Galactose was then added to induce rereplication, and at *T* = 3 hr cells were plated again to quantify the frequency of Lys$^+$ and Can^R mutants after rereplication. Induced mutation rates were calculated from the difference in mutant frequencies between *T* = 3 and *T* = 0 hr. Rereplication dependence was determined by measuring induced mutation rates after dextrose (which represses rereplication) is added instead of galactose or by measuring induced mutation rates in congenic control nonrereplicating strains (*orc6-cdk1A MCM7-2NLS pGAL*, see text) that have just the *pGAL* promoter instead of *pGAL-Δntcdc6-2A*. (B) Elevated frameshift reversion rate of *lys2InsE$_{A14}$* reporter is induced by rereplication and corresponds to the degree of rereplication. Basal and galactose-induced *lys2InsE$_{A14}$* frameshift mutation rates (mean ± SEM, *n* = 4–16, Table S4) for rereplicating (blue bars) and nonrereplicating (orange bars) strains were measured at the four sites shown in Figure 1A. Fold changes for induced *vs.* basal rates that have a *P*-value < 0.01 by the Mann–Whitney *U*-test are indicated above the bars. (C) Rereplication induces little increase in the mutation rate of the *CAN1* reporter. Mutation rates and fold changes for the *CAN1* reporter are displayed as in (B) (mean ± SEM, *n* = 3–9, Table S7). B, basal mutation rate; CAN, canavanine; I, galactose-induced mutation rate; SDC, synthetic complete dextrose media; YPRaff, yeast extract, peptone, raffinose media.

lower (12-fold). Further away, at sites 3 and 4, where there is little or no detectable rereplication, the *lys2InsE$_{A14}$* reporter showed no significant increase (*P*-value > 0.01) in reversion rate above basal rates (Figure 2B and Table S4). Control strains that do not rereplicate in the presence of galactose also displayed no significant increase (*P*-value > 0.01) over basal reversion rates at all four reporter sites (Figure 2B and Table S4). Thus, there was a correspondence between the amount of rereplication experienced by the *lys2InsE$_{A14}$* reporter and the amount of Lys$^+$ reversion induced. In contrast, the level of rereplication-induced gene amplification was similar regardless of the position of the *lys2InsE$_{A14}$* reporter, confirming that the overall effect of rereplication on the chromosome was the same for all reporters (Figure S2 and Table S5). Finally, *lys2InsE$_{A10}$*, a frameshift reporter containing a smaller A10 homopolymeric tract, also exhibited a significant degree of rereplication-induced Lys$^+$ reversion (18-fold; *P*-value < 0.01) when inserted at site 1 (Figure S3 and Table S6). Together, these results suggest that the passage of a rereplication fork can induce frameshift mutations.

Rereplication-induced mutagenesis can be exposed by compromising exonuclease proofreading

The *CAN1* reporter exhibited a small rereplication-induced increase in reversion rate at site 1 (Figure 2C and Table S7). This fourfold increase had a *P*-value < 0.01 based on the Mann–Whitney *U*-test and was not seen at site 1 for its congenic nonrereplicating control strain. However, the significance of this induced mutation rate was somewhat clouded by the roughly equivalent increases (albeit with *P*-value ≥ 0.01) seen in the nonrereplicating strains at sites 2 and 4. What is clear is that the *CAN1* reporter did not show the same degree of rereplication-induced mutagenesis as the *lys2InsE$_{A14}$* reporter.

The difference in results for the two reporters could be due to the fact that frameshift errors in long homopolymeric runs, like A14 in the *lys2InsE$_{A14}$* reporter, are poor substrates for

proofreading by replicative DNA polymerases (Tran *et al.* 1997; Deem *et al.* 2011). Unpaired nucleotides resulting from such frameshifts can be displaced away from the 3′ end of the primer-template junction, where proofreading polymerases sense and correct mismatches. Consequently, the *lys2InsE$_{A14}$* reporter is a highly sensitized frameshift reporter for detecting defects in nonproofreading fidelity mechanisms. In contrast, the general mutations detected by the *CAN1* reporter are readily proofread by replicative DNA polymerases. Hence, the discrepancy between the rereplication-induced mutagenesis of the *lys2InsE$_{A14}$* and *CAN1* reporters suggests that the proofreading of nucleotide misincorporations in *CAN1* may be masking the impaired rereplication fidelity detected by the *lys2InsE$_{A14}$* reporter.

To test this hypothesis, we reexamined the mutagenesis of *CAN1* when the proofreading function of the replisome was compromised. Pol ε and Pol δ are responsible, respectively, for synthesizing the leading and lagging daughter strands at the replication fork [reviewed in Burgers and Kunkel (2017)]. Budding yeast can tolerate inactivation of one but not both of their proofreading exonuclease activities (Morrison and Sugino 1994). Because Pol δ has a prominent role in break-induced repair through homologous recombination [reviewed in McVey *et al.* (2016)] and has been implicated *in vivo* in extrinsic exonuclease proofreading for other polymerases (Pavlov *et al.* 2006; Flood *et al.* 2015), its proofreading function may be less confined to the replisome. Hence, we repeated our *CAN1* mutagenesis analysis in the presence of a *pol2-4* mutation, which specifically disrupts the exonuclease activity of Pol ε (Morrison *et al.* 1991).

Consistent with the redundancy of replication fidelity mechanisms and as reported by others (Tran *et al.* 1997, 1999), the basal mutation rate of the *lys2InsE$_{A14}$* and *CAN1* reporters increased by only two- and fivefold, respectively, in the *pol2-4* background (Figure 3, and Tables S8 and S9). This higher basal mutation rate is reflected in the change in scale of the *y*-axis of Figure 3 compared to that in Figure 2. Given that frameshifts in the *lys2InsE$_{A14}$* A14 tract are already poorly proofread, it was not surprising that the rereplication-induced increase in Lys$^+$ reversion rate was not greatly affected by the addition of the *pol2-4* allele. The induced reversion rate changed by only a factor of two at site 1 (from 15-fold to 31-fold) and did not change significantly at site 2 (from 12-fold to 11-fold) (Figure 3B and Table S8). As expected, the frequency of rereplication-induced gene amplification also did not change much (Figure S4 and Table S10). However, for the *CAN1* reporter there was an obvious rereplication-induced increase in the mutation rate relative to the basal rate for both sites 1 and 2 (13-fold and eightfold, respectively) (Figure 3B and Table S9). Normalizing for 50% rereplication at site 1 yields a rereplication-induced increase in *CAN1* mutagenesis of 26-fold. Such an increase lends credence to the small and statistically significant increase in *CAN1* mutagenesis observed at site 1 in the wild-type *POL2* background (Figure 2C). Thus, the fidelity of DNA synthesis is compromised during rereplication, but much of this effect

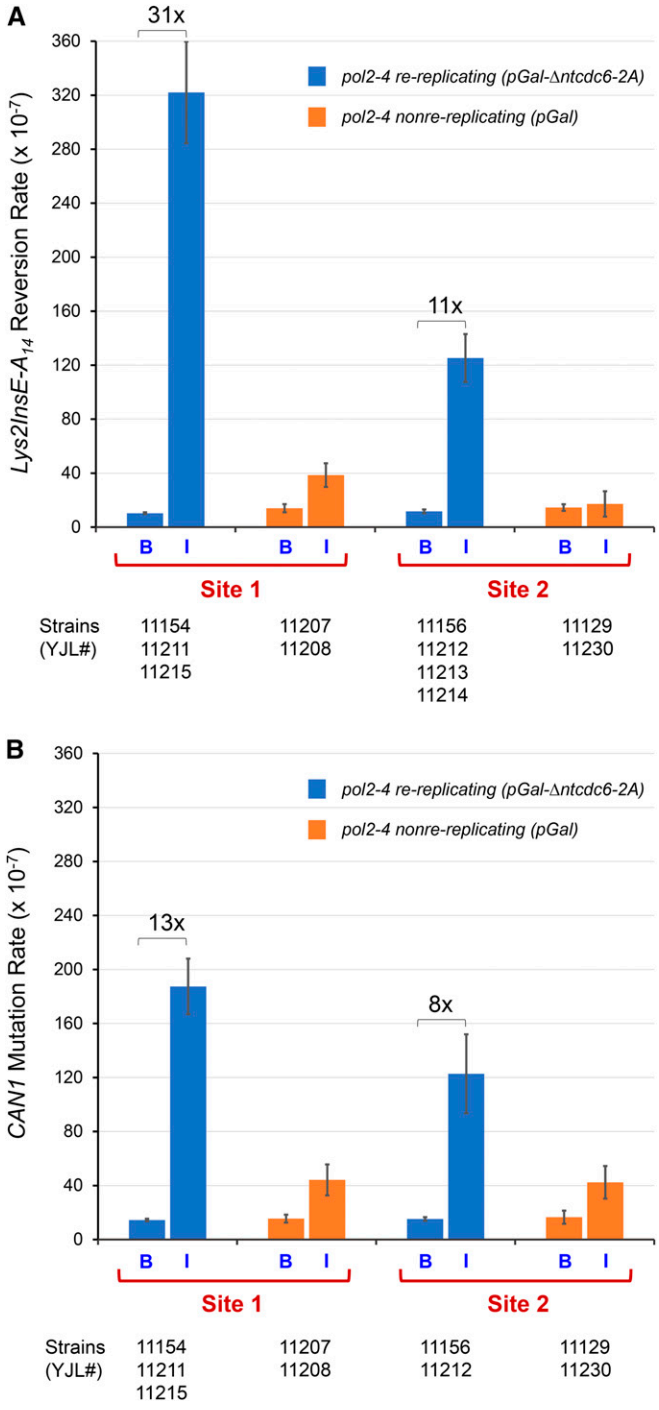

Figure 3 Rereplication increases the reversion rates of the *lys2InsE$_{A14}$* reporter and the mutation rate of the *CAN1* reporter when proofreading is compromised. Mutation rates were measured as described in Figure 2A, except in a Pol ε proofreading-defective strain background (*pol2-4*), and only at sites 1 and 2 (see Figure 1A). Fold changes for induced *vs.* basal rates that have a *P*-value < 0.01 by the Mann–Whitney *U*-test are indicated above the bars. (A) Basal and galactose-induced frameshift reversion rate of *lys2InsE$_{A14}$* (mean ± SEM, n = 5–25, Table S8). (B) Basal and galactose-induced mutation rate of *CAN1* (mean ± SEM, n = 5–15, Table S9). B, basal mutation rate; I, galactose-induced mutation rate.

can be masked by redundancy in error correction provided by DNA polymerase proofreading.

Rereplication-induced mutagenesis is not an indirect consequence of rereplication-induced breaks

We have previously reported that the rereplication forks that we induce are highly susceptible to breakage (Finn and Li 2013). In that report, we quantified the amount of rereplication-induced double-stranded breaks starting ~50-kb away from *ARS317* (near site 2) and extending further out. At these distances from the reinitiating origin, this break profile parallels the rereplication profile. Hence, for sites 2–4, the level of rereplication-induced mutagenesis not only corresponds to the level of rereplication, but also to the level of rereplication-induced breaks. Several studies have shown that DNA break repair through various homologous recombination mechanisms (gene conversion, gene conversion with gap repair, and break-induced replication) are error-prone, increasing reporter mutagenesis by as much as hundreds to thousands of fold (Strathern *et al.* 1995; Hicks *et al.* 2010; Deem *et al.* 2011). Thus, we had to consider the possibility that the rereplication-induced mutagenesis we observed might be secondary to rereplication fork breakage.

To separate the effect of rereplication *per se* from rereplication fork breakage, we examined the reversion rate of the *lys2InsE$_{A14}$* reporter in the subpopulation of sister chromatids that had undergone RRIGA. As discussed above, we can select for sister chromatids that have amplified a 124-kb segment encompassing the reinitiation origin *ARS317* and the two reporter sites closest to this origin. At the boundaries of this amplified segment, inserted at positions 521 and 645 kb of chromosome IV, are two fragments of the selectable *URA3* genes with 390 bp of overlapping sequence identity. As we previously showed (Finn and Li 2013), RRIGA occurs when bidirectional rereplication forks emanating from *ARS317* progress beyond both *URA3* fragments before breaking (Figure 4A). Nonallelic homologous recombination mediated by single-strand annealing between the rereplicated *URA3* fragments closest to the breakpoints then results in tandem duplication of the segment and reconstitution of a complete *URA3* gene at the boundary between segments.

Based on this mechanism of RRIGA, we inferred that the rereplication profile of sister chromatids that experienced RRIGA would show full and equal rereplication throughout the entire amplified segment before declining beyond its boundaries (Figure 4A). Importantly, rereplication fork breakage in this subpopulation of sister chromatids is excluded from within the amplified segment and clustered in two zones flanking the segment (Figure 4A). The *lys2InsE$_{A14}$* reporter inserted at site 1 is positioned toward the middle of this 124 kb-segment far away from these breaks, while the reporter inserted at site 2 is positioned ~10-kb away from the right boundary, closer to the zone of fork breakage. Hence, if passage of the rereplication fork were responsible for the rereplication-induced mutagenesis, we would expect the increase in *lys2InsE$_{A14}$* reversion rates for sister chromatids that experience RRIGA to be (1) equivalent at the two sites and (2) comparable to that for the bulk population of sister chromatids. On the other hand, if rereplication fork breakage were primarily responsible for the rereplication-induced mutagenesis, we would expect (1) the increase in *lys2InsE$_{A14}$* reversion rate at site 1 to be much lower in sister chromatids experiencing RRIGA than in the bulk population, and (2) the increase in *lys2InsE$_{A14}$* reversion rate at site 2 to be equivalent or higher than site 1 in cells experiencing RRIGA.

To quantify the sister chromatids that were induced by rereplication to undergo both RRIGA and reversion of the *lys2InsE$_{A14}$* reporter, we selected for cells that were both Ura$^+$ and Lys$^+$. For better statistical reliability, we performed these experiments in a *pol2-4* background to increase the number of rare Ura$^+$ Lys$^+$ cells present before rereplication induction. For the bulk population of *pol2-4* cells, rereplication induces a 31- and 11-fold higher reversion rate of *lys2InsE$_{A14}$* at site 1 and site 2, respectively (Figure 3A). After normalizing for 50% rereplication of site1 and 25% rereplication of site 2 (Figure 1A), this induction comes out to 62-fold for site 1 and 44-fold for site 2. Figure 4B and Table S11 show the rereplication-induced *lys2InsE$_{A14}$* reversion rate for the subpopulation of sister chromatids that experienced RRIGA. For this subpopulation, rereplication increases the *lys2InsE$_{A14}$* reversion rate by 81-fold for site 1 and 71-fold for site 2. These inductions are similar to each other and, despite the dearth of nearby rereplication fork breakage, comparable to the inductions for the bulk population. We conclude that the *lys2InsE$_{A14}$* reversion arises from passage of the rereplication fork and not from rereplication-induced breaks.

Rereplication induces both simple frameshift mutations and base substitutions

To examine the nature of the mutations induced during rereplication, we sequenced the *lys2InsE$_{A14}$* reporter for a subset of the Lys$^+$ revertants from YJL11215, a rereplicating *pol2-4* strain with the reporter inserted at site 1. All 11 of the spontaneous Lys$^+$ revertants and 16 out of 17 of the rereplication-induced Lys$^+$ revertants had a -1A frameshift mutation in the A14 homopolymeric tract. The one exception had a -1C frameshift mutation immediately after the homopolymeric tract. This result confirmed that both the spontaneous and rereplication-induced Lys$^+$ revertants in our strains occur through a simple frameshift, consistent with previous observations (Tran *et al.* 1997) and most readily explained by uncorrected replication slippage.

Notably, none of these frameshift mutations were accompanied by nearby base substitutions, a strong signature of frameshifts generated by DNA polymerase ζ (Pol ζ) in a similar *LYS2* frameshift assay (Harfe and Jinks-Robertson 2000). This error-prone polymerase is responsible for much of the spontaneous and DNA damage-induced mutagenesis in budding yeast, and has been implicated in mutagenesis associated with replication stress and break repair (Lawrence 2004; Northam *et al.* 2014; Makarova and Burgers 2015; McVey *et al.* 2016). However, our sequence data suggest that it does not play a

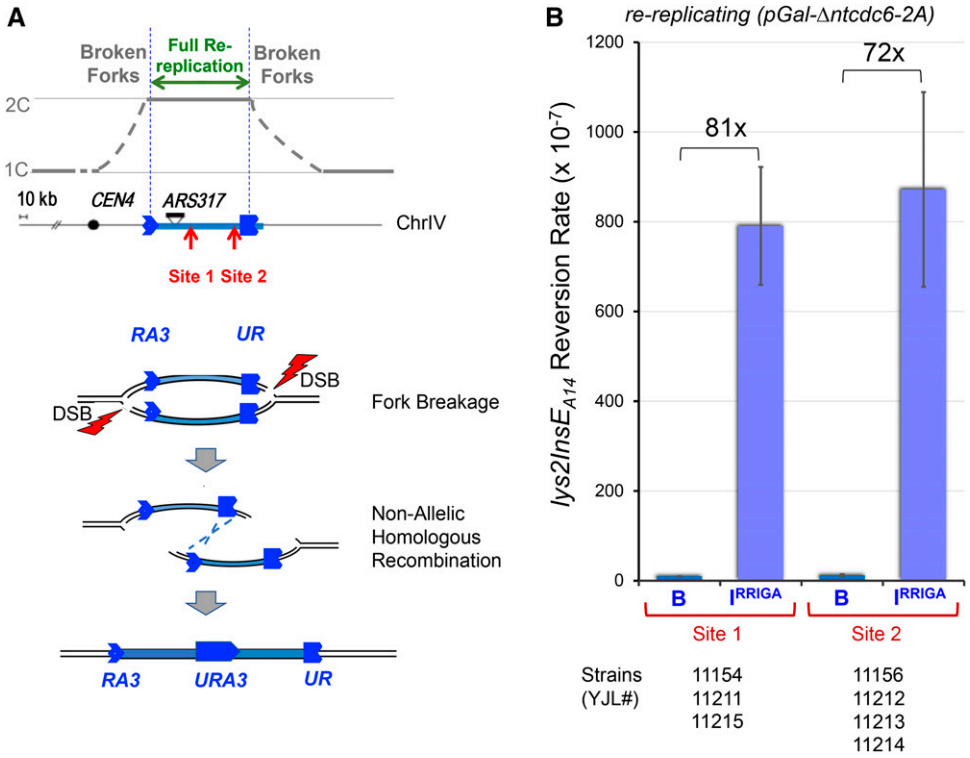

Figure 4 Rereplication-induced mutagenesis of *lys2InsE$_{A14}$* correlates with rereplication and is independent of rereplication-induced breaks. (A) Rereplication profile and location of rereplication-induced breaks for the subpopulation of chromosome IV (ChrIV) sister chromatids that underwent rereplication-induced gene amplification (RRIGA). Profile is inferred from the mechanism of amplification shown below (Finn and Li 2013), which requires (i) that rereplication forks emanating from *ARS317* rereplicate the entire amplified segment (copy number = 2C); (ii) that the forks start to stall and break in *trans* distal to the *RA3* and *UR* RRIGA reporter fragments; and (iii) that the breaks be repaired by homologous recombination between these fragments. Positions on chromosome IV of *CEN4*, reinitiating *ARS317*, split *URA3* amplification reporter fragments, and mutagenesis reporters inserted at sites 1 and 2 are the same as in Figure 1A. (B) Galactose-induced reversion rate of *lys2InsE$_{A14}$* (mean ± SEM, *n* = 11–15, Table S11) in the subpopulation of sister chromatids that underwent RRIGA (I^{RRIGA}) compared to the basal (B) reversion rate of *lys2InsE$_{A14}$*. Assay performed as described in Figure 2A, except Ura$^+$ Lys$^+$ mutants were also quantified and used to calculate I^{RRIGA} as described in the *Materials and Methods*. DSB, double-strand break.

major role in rereplication-induced mutagenesis, and we have confirmed this directly by deletion analysis (see below).

We also sequenced the *can1^R* alleles from reporters at site 1 (YJL11215) and site 2 (YJL11213 and YJL11214), both before and after the induction of rereplication in the *pol2-4* background (Table S12). With the exception of one double-base pair substitution 12-nt apart, these mutations consisted of single-base pair substitutions or single-base pair frameshifts scattered throughout the *CAN1* coding sequence (Figure 5). Most of the frameshift mutations were observed in small homonucleotide runs, again suggestive of uncorrected replication slippage events. Together, the sequence analyses of the two mutagenesis reporters are consistent with error correction being partially compromised during rereplication.

Rereplication induces mutagenesis by compromising MMR

Like replication, rereplication is subject to three error-avoidance mechanisms working in series and cooperating in a multiplicative manner to reduce the rate of nucleotide misincorporation: nucleotide selectivity during the initial incorporation, proofreading, and MMR. One model for how the fidelity of rereplication could be less than the fidelity of replication is that one (or more) of these mechanisms is compromised during rereplication. If we disrupt that mechanism, the fidelity of both replication and rereplication would be equally compromised, precluding the induction of a higher mutation rate by rereplication. On the other hand, if the disrupted mechanism is not the one compromised by rereplication, then we should still observe rereplication-induced mutagenesis, albeit starting from a higher basal rate.

The fact that rereplication induces significant mutagenesis in the proofreading-defective *pol2-4* strain background directed us toward nucleotide selectivity and/or MMR as the possible error-avoidance mechanism(s) impaired by rereplication. To test whether MMR is impaired, we quantified the basal and rereplication-induced reversion rate of *lys2InsE$_{A14}$* at site 1 in an *msh2*Δ background, which ablates MMR. Similar to previous reports, the basal *lys2InsE$_{A14}$* reversion rates in the *msh2*Δ strains increased by several thousand-fold (Tran *et al.* 1997). However, the induction of a 15-fold higher reversion rate by rereplication was lost, resembling the lack of induction observed when rereplication is prevented (Figure 6 and Table S13). A similar result was observed if MMR was crippled using an *mlh1*Δ deletion instead of *msh2*Δ (Figure S5A and Table S14). Both deletion backgrounds still induced robust increases in Ura+ rates (Figure S6A, and Tables S15 and S16), suggesting that these deletions do not perturb the induction of rereplication nor its expected stimulation of amplification. Together, these results raise the possibility that rereplication-induced mutagenesis operates primarily through the impairment of MMR. However, one can imagine three alternative explanations that require consideration.

One is that we failed to see a rereplication-induced increase in the *lys2InsE$_{A14}$* reversion rate because the overall error rate caused by the loss of MMR function is near the limit of what

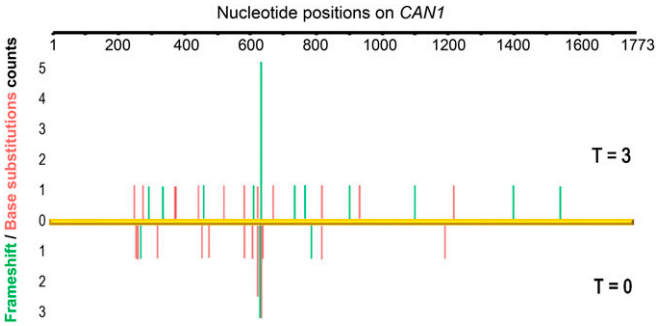

Figure 5 Location of *can1*-inactivating mutations found in canavanine resistant (Can^R) strains. Can^R mutants obtained from the *pol2-4* experiment described in Figure 3 were sequenced to identify mutations in the *CAN1* coding sequence (Table S12). The number of frameshift (green) and base substitution (red) mutations at each nucleotide position are displayed. Top: Can^R mutations isolated after the induction of rereplication. Bottom: Can^R mutations acquired before the induction of rereplication.

cells can tolerate due to error-induced extinction. Indeed, an upper limit for the reversion rate of the *lys2InsE$_{A14}$* reporter in budding yeast can be observed as an increasing number of fidelity mechanisms are genetically ablated, eventually resulting in lethality (Tran *et al.* 1999). However, this limit is at least five times higher than the reversion rate in an *msh2*Δ strain (Tran *et al.* 1999). Moreover, even this fivefold limit may not apply to our experiments, as our transient and limited pulse of rereplication does not cause any increased inviability in the MMR mutant strains (data not shown). In other words, the rereplication in our experiments is not pushing the MMR mutant strains over the threshold for error-induced extinction.

A second alternative possibility is that there is some intrinsic saturation of the *lys2InsE$_{A14}$* reversion assay, and we are approaching the saturation limit in the MMR mutants. To address this possibility, we examined rereplication-induced *CAN1* mutagenesis in the MMR mutants. In contrast to *lys2InsE$_{A14}$* reversion, the basal rate of Can^R generation increases only 20–70-fold in MMR mutants (Figure S5B, and Tables S17 and S18) (Johnson *et al.* 1996; Marsischky *et al.* 1996; Shcherbakova and Kunkel 1999; Tran *et al.* 1999) and has room to increase ~50-fold more before being limited by error-induced extinction (Tran *et al.* 1999). As discussed previously, in MMR-proficient cells rereplication induces a small (fourfold) but reproducible increase in the *CAN1* mutation rate at site 1 (Figure 2C). Despite the large dynamic range still available to the *CAN1* reporter, this induction was lost in both an *msh2*Δ and an *mlh1*Δ background (Figure S5B, and Tables S17 and S18). These results argue against assay saturation being the underlying cause for the loss of the rereplication-induced mutagenesis in the MMR mutant background.

The third alternative possibility to explain the disappearance of rereplication-induced mutagenesis in MMR mutants is that rereplication induces mutagenesis through a mechanism that does not operate in series with MMR. In such a situation, the increase in mutagenesis from rereplication and MMR disruption would cooperate in an additive rather than multiplicative manner, and the small increase from rereplication could be eclipsed by the larger increase due to MMR disruption. The predominant replication-associated mechanism that is known to act in such an additive fashion is mutagenesis by the error-prone polymerase Pol ζ. Pol ζ is enlisted in response to stalled or stressed replication repair (Lawrence 2004; Northam *et al.* 2014; Makarova and Burgers 2015; McVey *et al.* 2016), but its errors do not appear to be subject to MMR correction (Huang *et al.* 2002; Lehner and Jinks-Robertson 2009; Aksenova *et al.* 2010; Kochenova *et al.* 2015). As discussed earlier, our sequencing of rereplication-induced *can1^R* mutations suggested that Pol ζ might not be responsible for generating these mutations. More direct analysis by deletion of *REV3*, which encodes the catalytic subunit of Pol ζ, indicates that the rereplication-induced mutagenesis of both *lys2InsE$_{A14}$* and *CAN1* does not require Pol ζ (Figure 7, and Tables S19 and S20). As with previous deletion mutants, control experiments confirm that RRIGA is induced normally in the *rev3*Δ strains (Figure S7 and Table S21).

Taken together, these results reinforce the notion that rereplication is likely inducing mutagenesis by compromising one or more of the three sequential error-avoidance mechanisms that ensure replication fidelity. Thus, the simplest explanation for why this induction is lost in the MMR mutants is because this induction arises from partial impairment of MMR.

Discussion

A wider effect of rereplication on genome stability

We have previously shown that rereplication is an extremely potent source of gross chromosomal rearrangements such as gene amplification (Green *et al.* 2010; Finn and Li 2013) and whole-chromosome aneuploidy (Hanlon and Li 2015). In this study, we establish that rereplication also makes cells more prone to nucleotide-level mutagenesis, broadening the consequences of rereplication on genome stability. Thus, mechanisms important for the control of replication initiation also contribute to the fidelity of DNA synthesis.

The effect of rereplication on nucleotide-level mutagenesis is less dramatic than its effect on gross chromosomal rearrangements and can be masked by the partial redundancy of replication fidelity mechanisms. However, when we alleviated this redundancy by using the proofreading-resistant *lys2InsE$_{A14}$* reporter or by inactivating the proofreading exonuclease of Pol ε for the *CAN1* reporter, we observed a 26–30-fold increase in the rate of frameshift and/or base substitutions. As discussed below, such a moderate effect on the fidelity of DNA synthesis may be relevant to the accumulation of mutations in cancers.

How does rereplication compromise nucleotide fidelity?

Given that rereplication forks show increased susceptibility to breakage and that recombinational repair of double-strand breaks has been associated with mutagenesis [reviewed in Malkova and Haber (2012)], one trivial reason for

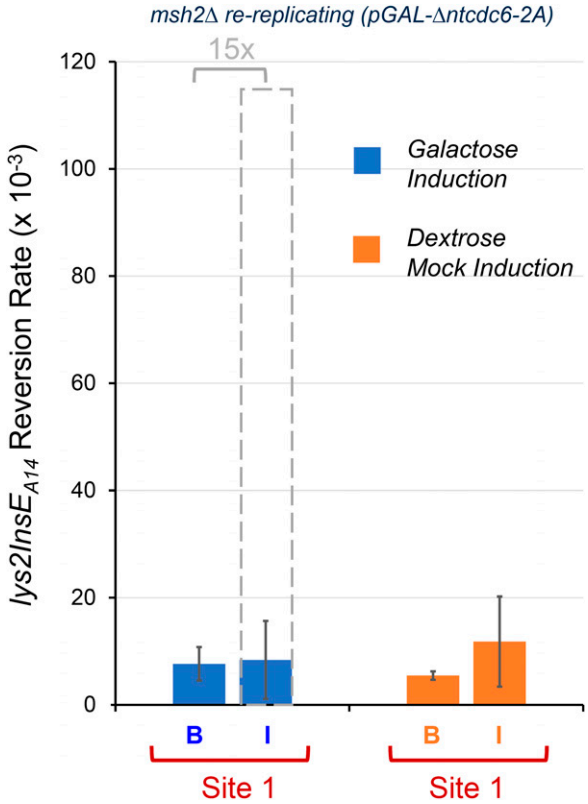

Figure 6 Rereplication does not induce *lys2InsE$_{A14}$* reversions when mismatch repair (MMR) is compromised. Frameshift reversion rates of *lys2InsE$_{A14}$* were measured as described in Figure 2A in rereplicating strains (YJL11234, YJL11235, and YJL11236) that are MMR null (*msh2*Δ) and have a mutagenesis reporter cassette inserted at site 1 (see Figure 1A). The dotted column represents what the induced reversion rate would be if the ratio of induced to basal reversion rates matched the 15× ratio observed in the *MSH2* strains (Figure 2B). As discussed in the text, this ratio is what one would expect if rereplication reduces fidelity by compromising an error-avoidance mechanism distinct from and working in series with MMR, *e.g.*, nucleotide selectivity or proofreading. Basal (B) and galactose-induced (I) rates are shown for rereplicating conditions (mean ± SEM, $n = 24$, Table S13). Basal (B) and dextrose-induced (I) rates are shown for nonrereplicating conditions (mean ± SEM, $n = 8$, Table S13). For both conditions, the difference between induced and basal rates has a *P*-value > 0.1 by the Mann–Whitney *U*-test.

rereplication-induced mutagenesis is increased break repair. However, when we required a large 124-kb segment to be rereplicated intact by selecting for rereplication events that result in amplification of the segment, we saw no decrease in mutation rate for reporters within that segment. Thus, the extent of mutagenesis correlates with the level of rereplication and not with the level of fork breakage, arguing that the mutagenesis occurred during DNA synthesis by the rereplication fork.

Our inquiry of how rereplication forks might generate an elevated error rate was directed by our understanding of how errors are generated and handled during DNA replication. Three error-avoidance mechanisms that cooperate in a multiplicative manner to reduce the error rate of DNA replication—polymerase nucleotide selectivity, polymerase proofreading, and MMR—are also available to reduce the error rate during rereplication. Compromising one or more of these mechanisms could provide one way in which rereplication could increase mutations rates. In principle, mutations can also be generated during DNA rereplication by recruitment of the error-prone DNA polymerase, Pol ζ, which is responsible for much of the mutations that arise spontaneously, or in response to DNA damage or replication stress in budding yeast (Lawrence 2004; Northam *et al.* 2014; Makarova and Burgers 2015; McVey *et al.* 2016). However, our finding that *REV3*, the gene encoding the catalytic subunit of Pol ζ, is not required for rereplication-induced mutagenesis argues against this possibility. Given this result, the loss of rereplication-induced mutagenesis in MMR mutant backgrounds suggests that this mutagenesis arises primarily by compromising MMR.

Future studies will be needed to determine how MMR might be compromised during rereplication. We offer one suggestion based on the prevailing notion that eukaryotic DNA replication and MMR are somehow coupled [reviewed in Kunkel and Erie (2015)]. This coupling is conceptually appealing because MMR requires replacement of mismatched sequences specifically on the daughter strand, which is most readily distinguished from parental strands at newly replicated DNA. Two types of observations have encouraged this notion: (1) the temporal and spatial association of MMR with DNA replication in eukaryotic cells (Kleczkowska *et al.* 2001; Hombauer *et al.* 2011a,b), and (2) the interaction of MMR proteins with PCNA (Clark *et al.* 2000; Flores-Rozas *et al.* 2000; Dzantiev *et al.* 2004; Lee and Alani 2006), the sliding clamp for Pol ε and Pol δ. PCNA, we note, is loaded around replicating DNA with an orientation specified by which strand is the daughter strand [reviewed in Modrich (2016)], so, in principle, PCNA can remember daughter strand identity and transmit this information to interacting MMR proteins. In budding yeast, the two MMR complexes that first bind and recognize mismatched DNA, Msh2-Msh6 and Msh2-Msh3, also bind PCNA (Clark *et al.* 2000; Flores-Rozas *et al.* 2000). Later, daughter-specific strand excision of the mismatched segment is facilitated by Mlh1-Pms1, whose endonuclease-nicking activity is directed to daughter strands through its interaction with PCNA (Pluciennik *et al.* 2010). These molecular connections hint at coordination between DNA replication and MMR designed to enhance the efficiency of the latter. We speculate that this coordination may somehow be suboptimal during DNA rereplication, causing indirect attenuation of MMR.

Possible role of weak MMR defects in cancer

More than 40 years ago, Loeb proposed that an increase in mutation rate, which he termed a mutator phenotype, could promote tumor initiation and/or progression (Loeb 2016). Strong MMR defects arising from genetic or epigenetic inactivation of key MMR genes (*e.g.*, *hMSH2* and *hMLH1*) provided the first validation of this hypothesis (Fishel and

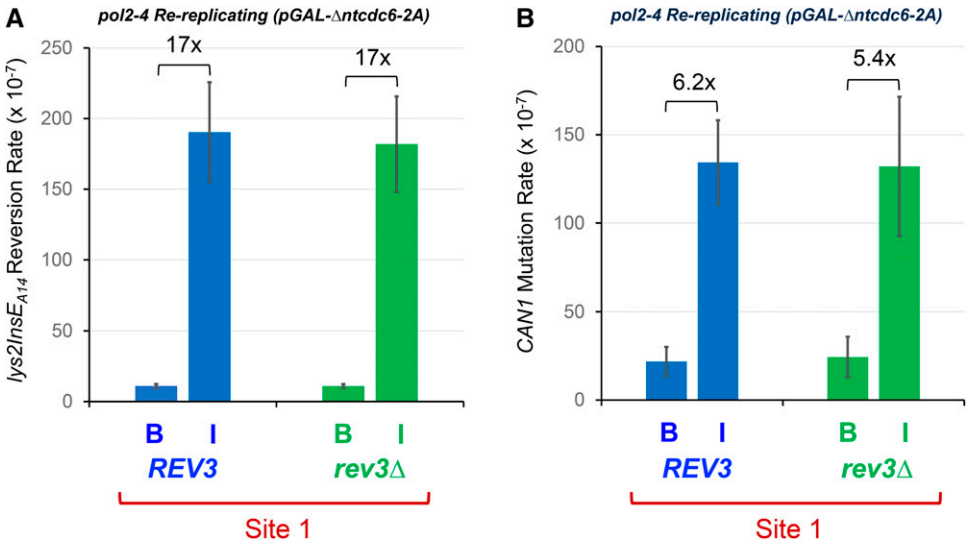

Figure 7 Rev3 is not required for rereplication-induced mutagenesis. Rereplicating strains (*orc6-cdk1A MCM7-2NLS pGAL-Δntcdc6-2A*) containing the *pol2-4* allele, and either wild-type *REV3 (YJL11154)* or *rev3Δ (YJL11324-11326)*, were induced to undergo rereplication as described in Figure 2A. Mutation rates were measured using the *CAN1-lys2InsE$_{A14}$* mutagenesis reporter cassette inserted at site 1 (see Figure 1A). (A) Basal (B) and galactose-induced (I) rates (mean ± SEM, n = 6) of *lys2-InsE$_{A14}$* reversion (Lys$^+$, Table S19). (B) Basal (B) and galactose-induced (I) rates (mean ± SEM, n = 6) of *CAN1* mutation (Can^R, Table S20). Fold changes with P-value < 0.01 by the Mann–Whitney U-test are shown. Can, canavanine.

Kolodner 1995; Kinzler and Vogelstein 1996; Modrich 2016). These defects generate a mutator phenotype (detected as a high level of microsatellite repeat instability or MSI-H) that is responsible for a small subset of colorectal, endometrial, and stomach cancers. Many of these cancers appear as part of Lynch syndrome, an inherited disorder where germline inactivation of MMR genes causes a strong familial susceptibility to early cancer development [reviewed in Peltomäki (2016)].

Recent findings suggest that weaker MMR defects with subtler mutator phenotypes may be associated with a broader range of cancers. Diagnostic sequencing of suspected Lynch syndrome patients, whose cancers exhibit low penetrance and/or late occurrence, has identified a growing number of missense mutations that have uncertain functional consequences in MMR genes. Assays attempting to assess the pathogenicity of these "variants of uncertain clinical significance" often show weak MMR defects (Heinen and Juel Rasmussen 2012; Wielders *et al.* 2014; Peltomäki 2016). This has led to speculation that weak MMR defects, possibly in synergism with other weak repair defects, generate enough of a mutator phenotype to promote sporadic cancers (Liccardo *et al.* 2017). Importantly, even if a cancer is initiated by other means, its progression or eventual therapeutic resistance might still be facilitated by a weak MMR defect.

Whole-exome and whole-genome sequencing of thousands of cancer samples suggests that such weak mutator phenotypes may be more prevalent than previously realized (Hause *et al.* 2016; Cortes-Ciriano *et al.* 2017). These studies reveal a broad and continuous range in the number of microsatellite alterations present in cancers, with many cancer samples displaying moderate to low amounts. Interestingly, some of these samples have no detectable genetic or epigenetic defects in MMR genes (Cortes-Ciriano *et al.* 2017), raising the possibility that MMR in these cancers is somehow attenuated by indirect means.

Another potential role of rereplication in tumor biology

Our observation that MMR is compromised during rereplication offers one possible means for the indirect attenuation of MMR in cancer. This possibility is encouraged by growing circumstantial evidence that rereplication occurs in some cancers. First, moderately elevated levels of the replication initiation proteins Cdc6 and Cdt1, which in high amounts induce overt rereplication in cell culture and model organisms, has been observed in several types of primary human tumors (Karakaidos *et al.* 2004; Liontos *et al.* 2007). Such widespread overexpression may be due in part to the fact that the Rb-E2F pathway, which controls *CDC6* and *CDT1* transcription (Truong and Wu 2011), is often deregulated in cancer cells (Vogelstein and Kinzler 2004). Second, moderate overexpression of Cdc6 and Cdt1 can potentiate oncogenesis in mouse models (Arentson *et al.* 2002; Seo *et al.* 2005; Liontos *et al.* 2007). Overt rereplication was not detected in these experiments, as expected given that currently detectable levels of rereplication are associated with extensive DNA damage and cell lethality (Vaziri *et al.* 2003; Melixetian *et al.* 2004; Zhu *et al.* 2004; Archambault *et al.* 2005; Green and Li 2005; Jin *et al.* 2006; Green *et al.* 2010; Hanlon and Li 2015). However, the possibility remains open that rereplication does occur in these and other cancer cells, but at low levels that are both currently undetectable and compatible with viability.

Our previous finding that rereplication efficiently induces gross chromosomal alterations has provided a potential source for these alterations in cancers. For example, rereplication has been speculated to contribute to the large number of tandem segmental duplications (tandem duplicator phenotype) observed in a subset of breast, ovarian, and endometrial carcinomas (Menghi *et al.* 2016). The results described here suggest that rereplication may also be relevant to some of the extensive nucleotide-level mutagenesis observed in cancers (Hollstein *et al.* 2017).

Acknowledgments

The authors thank Bruce Futcher for providing the CRISPR-Cas9 plasmid and Dmitry Gordenin for providing the *lys2InsE* frameshift reporters. Work in the laboratory of J.J.L. is supported by National Institutes of Health grant RO1 GM-059704.

Literature Cited

Abbas, T., M. A. Keaton, and A. Dutta, 2013 Genomic instability in cancer. Cold Spring Harb. Perspect. Biol. 5: a012914. https://doi.org/10.1101/cshperspect.a012914

Aksenova, A., K. Volkov, J. Maceluch, Z. F. Pursell, I. B. Rogozin *et al.*, 2010 Mismatch repair-independent increase in spontaneous mutagenesis in yeast lacking non-essential subunits of DNA polymerase epsilon. PLoS Genet. 6: e1001209. https://doi.org/10.1371/journal.pgen.1001209

Alexander, J. L., and T. L. Orr-Weaver, 2016 Replication fork instability and the consequences of fork collisions from rereplication. Genes Dev. 30: 2241–2252. https://doi.org/10.1101/gad.288142.116

Archambault, V., A. E. Ikui, B. J. Drapkin, and F. R. Cross, 2005 Disruption of mechanisms that prevent rereplication triggers a DNA damage response. Mol. Cell. Biol. 25: 6707–6721. https://doi.org/10.1128/MCB.25.15.6707-6721.2005

Arentson, E., P. Faloon, J. Seo, E. Moon, J. M. Studts *et al.*, 2002 Oncogenic potential of the DNA replication licensing protein CDT1. Oncogene 21: 1150–1158. https://doi.org/10.1038/sj.onc.1205175

Buckland, R. J., D. L. Watt, B. Chittoor, A. K. Nilsson, T. A. Kunkel *et al.*, 2014 Increased and imbalanced dNTP pools symmetrically promote both leading and lagging strand replication infidelity. PLoS Genet. 10: e1004846. https://doi.org/10.1371/journal.pgen.1004846

Bui, D. T., E. Dine, J. B. Anderson, C. F. Aquadro, and E. E. Alani, 2015 A genetic incompatibility accelerates adaptation in yeast. PLoS Genet. 11: e1005407. https://doi.org/10.1371/journal.pgen.1005407

Burgers, P. M. J., and T. A. Kunkel, 2017 Eukaryotic DNA replication fork. Annu. Rev. Biochem. 86: 417–438. https://doi.org/10.1146/annurev-biochem-061516-044709

Chattoo, B. B., F. Sherman, D. A. Azubalis, T. A. Fjellstedt, D. Mehnert *et al.*, 1979 Selection of lys2 mutants of the yeast SACCHAROMYCES CEREVISIAE by the utilization of alpha-AMINOADIPATE. Genetics 93: 51–65.

Chee, M. K., and S. B. Haase, 2012 New and redesigned pRS plasmid shuttle vectors for genetic manipulation of Saccharomyces cerevisiae. G3 (Bethesda) 2: 515–526. https://doi.org/10.1534/g3.111.001917

Clark, A., F. Valle, K. Drotschmann, R. K. Gary, and T. A. Kunkel, 2000 Functional interaction of proliferating cell nuclear antigen with MSH2–MSH6 and MSH2–MSH3 complexes. J. Biol. Chem. 275: 36498–36501. https://doi.org/10.1074/jbc.C000513200

Cortes-Ciriano, I., S. Lee, W. Y. Park, T. M. Kim, and P. J. Park, 2017 A molecular portrait of microsatellite instability across multiple cancers. Nat. Commun. 8: 15180. https://doi.org/10.1038/ncomms15180

Deem, A., A. Keszthelyi, T. Blackgrove, A. Vayl, B. Coffey *et al.*, 2011 Break-induced replication is highly inaccurate. PLoS Biol. 9: e1000594. https://doi.org/10.1371/journal.pbio.1000594

Drake, J., 1991 Spontaneous mutation. Annu. Rev. Genet. 25: 125–146. https://doi.org/10.1146/annurev.ge.25.120191.001013

Dzantiev, L., N. Constantin, J. Genschel, R. R. Iyer, P. M. Burgers *et al.*, 2004 A defined human system that supports bidirectional mismatch-provoked excision. Mol. Cell 15: 31–41. https://doi.org/10.1016/j.molcel.2004.06.016

Engel, S. R., F. S. Dietrich, D. G. Fisk, G. Binkley, R. Balakrishnan *et al.*, 2014 The reference genome sequence of Saccharomyces cerevisiae: then and now. G3 (Bethesda) 4: 389–398. https://doi.org/10.1534/g3.113.008995

Finn, K. J., and J. J. Li, 2013 Single-stranded annealing induced by re-initiation of replication origins provides a novel and efficient mechanism for generating copy number expansion via non-allelic homologous recombination. PLoS Genet. 9: e1003192. https://doi.org/10.1371/journal.pgen.1003192

Fishel, R., and R. D. Kolodner, 1995 Identification of mismatch repair genes and their role in the development of cancer. Curr. Opin. Genet. Dev. 5: 382–395. https://doi.org/10.1016/0959-437X(95)80055-7

Flood, C. L., G. P. Rodriguez, G. Bao, A. H. Shockley, Y. W. Kow *et al.*, 2015 Replicative DNA polymerase δ but not ε proofreads errors in Cis and in Trans. PLoS Genet. 11: e1005049. https://doi.org/10.1371/journal.pgen.1005049

Flores-Rozas, H., D. Clark, and R. D. Kolodner, 2000 Proliferating cell nuclear antigen and Msh2p-Msh6p interact to form an active mispair recognition complex. Nat. Genet. 26: 375–378. https://doi.org/10.1038/81708

Ganai, R. A., and E. Johansson, 2016 DNA replication-A matter of fidelity. Mol. Cell 62: 745–755. https://doi.org/10.1016/j.molcel.2016.05.003

Green, B. M., and J. J. Li, 2005 Loss of rereplication control in Saccharomyces cerevisiae results in extensive DNA damage. Mol. Biol. Cell 16: 421–432. https://doi.org/10.1091/mbc.e04-09-0833

Green, B. M., R. J. Morreale, B. Ozaydin, J. L. Derisi, and J. J. Li, 2006 Genome-wide mapping of DNA synthesis in Saccharomyces cerevisiae reveals that mechanisms preventing reinitiation of DNA replication are not redundant. Mol. Biol. Cell 17: 2401–2414. https://doi.org/10.1091/mbc.e05-11-1043

Green, B. M., K. J. Finn, and J. J. Li, 2010 Loss of DNA replication control is a potent inducer of gene amplification. Science 329: 943–946. https://doi.org/10.1126/science.1190966

Greene, C. N., and S. Jinks-Robertson, 2001 Spontaneous frameshift mutations in Saccharomyces cerevisiae: accumulation during DNA replication and removal by proofreading and mismatch repair activities. Genetics 159: 65–75.

Hanlon, S. L., and J. J. Li, 2015 Re-replication of a centromere induces chromosomal instability and aneuploidy. PLoS Genet. 11: e1005039. https://doi.org/10.1371/journal.pgen.1005039

Harfe, B. D., and S. Jinks-Robertson, 2000 DNA polymerase zeta introduces multiple mutations when bypassing spontaneous DNA damage in Saccharomyces cerevisiae. Mol. Cell 6: 1491–1499. https://doi.org/10.1016/S1097-2765(00)00145-3

Hause, R. J., C. C. Pritchard, J. Shendure, and S. J. Salipante, 2016 Classification and characterization of microsatellite instability across 18 cancer types. Nat. Med. 22: 1342–1350 [corrigenda: Nat. Med. 23: 1241 (2017)]; [corrigenda: Nat. Med. 24: 525 (2018)]. https://doi.org/10.1038/nm.4191

Heinen, C. D., and L. Juel Rasmussen, 2012 Determining the functional significance of mismatch repair gene missense variants using biochemical and cellular assays. Hered. Cancer Clin. Pract. 10: 9. https://doi.org/10.1186/1897-4287-10-9

Hicks, W. M., M. Kim, and J. E. Haber, 2010 Increased mutagenesis and unique mutation signature associated with mitotic gene conversion. Science 329: 82–85. https://doi.org/10.1126/science.1191125

Hollstein, M., L. B. Alexandrov, C. P. Wild, M. Ardin, and J. Zavadil, 2017 Base changes in tumour DNA have the power to reveal

the causes and evolution of cancer. Oncogene 36: 158–167. https://doi.org/10.1038/onc.2016.192

Hombauer, H., C. S. Campbell, C. E. Smith, A. Desai, and R. D. Kolodner, 2011a Visualization of eukaryotic DNA mismatch repair reveals distinct recognition and repair intermediates. Cell 147: 1040–1053. https://doi.org/10.1016/j.cell.2011.10.025

Hombauer, H., A. Srivatsan, C. D. Putnam, and R. D. Kolodner, 2011b Mismatch repair, but not heteroduplex rejection, is temporally coupled to DNA replication. Science 334: 1713–1716. https://doi.org/10.1126/science.1210770

Huang, M.-E., A.-G. Rio, M.-D. Galibert, and F. Galibert, 2002 Pol32, a subunit of Saccharomyces cerevisiae DNA polymerase delta, suppresses genomic deletions and is involved in the mutagenic bypass pathway. Genetics 160: 1409–1422.

Jin, J., E. E. Arias, J. Chen, J. W. Harper, and J. C. Walter, 2006 A family of diverse Cul4-Ddb1-interacting proteins includes Cdt2, which is required for S phase destruction of the replication factor Cdt1. Mol. Cell 23: 709–721. https://doi.org/10.1016/j.molcel.2006.08.010

Johnson, R. E., G. K. Kovvali, L. Prakash, and S. Prakash, 1996 Requirement of the yeast MSH3 and MSH6 genes for MSH2-dependent genomic stability. J. Biol. Chem. 271: 7285–7288. https://doi.org/10.1074/jbc.271.13.7285

Johnston, M., 1987 A model fungal gene regulatory mechanism: the GAL genes of Saccharomyces cerevisiae. Microbiol. Rev. 51: 458–476.

Karakaidos, P., S. Taraviras, L. V. Vassiliou, P. Zacharatos, N. G. Kastrinakis *et al.*, 2004 Overexpression of the replication licensing regulators hCdt1 and hCdc6 characterizes a subset of non-small-cell lung carcinomas: synergistic effect with mutant p53 on tumor growth and chromosomal instability–evidence of E2F–1 transcriptional control over hCdt1. Am. J. Pathol. 165: 1351–1365. https://doi.org/10.1016/S0002-9440(10)63393-7

Kinzler, K. W., and B. Vogelstein, 1996 Lessons from hereditary colorectal cancer. Cell 87: 159–170. https://doi.org/10.1016/S0092-8674(00)81333-1

Kleczkowska, H. E., G. Marra, T. Lettieri, and J. Jiricny, 2001 hMSH3 and hMSH6 interact with PCNA and colocalize with it to replication foci. Genes Dev. 15: 724–736. https://doi.org/10.1101/gad.191201

Kochenova, O. V., D. L. Daee, T. M. Mertz, and P. V. Shcherbakova, 2015 DNA polymerase zeta-dependent lesion bypass in Saccharomyces cerevisiae is accompanied by error-prone copying of long stretches of adjacent DNA. PLoS Genet. 11: e1005110. https://doi.org/10.1371/journal.pgen.1005110

Kunkel, T. A., 2009 Evolving views of DNA replication (in)fidelity. Cold Spring Harb. Symp. Quant. Biol. 74: 91–101. https://doi.org/10.1101/sqb.2009.74.027

Kunkel, T. A., and D. A. Erie, 2015 Eukaryotic mismatch repair in relation to DNA replication. Annu. Rev. Genet. 49: 291–313. https://doi.org/10.1146/annurev-genet-112414-054722

Lang, G. I., and A. W. Murray, 2008 Estimating the per-base-pair mutation rate in the yeast Saccharomyces cerevisiae. Genetics 178: 67–82. https://doi.org/10.1534/genetics.107.071506

Lawrence, C. W., 2004 Cellular functions of DNA polymerase zeta and Rev1 protein. Adv. Protein Chem. 69: 167–203. https://doi.org/10.1016/S0065-3233(04)69006-1

Lee, S. D., and E. Alani, 2006 Analysis of interactions between mismatch repair initiation factors and the replication processivity factor PCNA. J. Mol. Biol. 355: 175–184. https://doi.org/10.1016/j.jmb.2005.10.059

Lehner, K., and S. Jinks-Robertson, 2009 The mismatch repair system promotes DNA polymerase zeta-dependent translesion synthesis in yeast. Proc. Natl. Acad. Sci. USA 106: 5749–5754. https://doi.org/10.1073/pnas.0812715106

Liccardo, R., M. De Rosa, P. Izzo, and F. Duraturo, 2017 Novel implications in molecular diagnosis of lynch syndrome. Gastroenterol. Res. Pract. 2017: 2595098. https://doi.org/10.1155/2017/2595098

Liontos, M., M. Koutsami, M. Sideridou, K. Evangelou, D. Kletsas *et al.*, 2007 Deregulated overexpression of hCdt1 and hCdc6 promotes malignant behavior. Cancer Res. 67: 10899–10909. https://doi.org/10.1158/0008-5472.CAN-07-2837

Loeb, L. A., 2016 Human cancers express a mutator phenotype: hypothesis, origin, and consequences. Cancer Res. 76: 2057–2059. https://doi.org/10.1158/0008-5472.CAN-16-0794

Lujan, S. A., J. S. Williams, Z. F. Pursell, A. A. Abdulovic-Cui, A. B. Clark *et al.*, 2012 Mismatch repair balances leading and lagging strand DNA replication fidelity. PLoS Genet. 8: e1003016. https://doi.org/10.1371/journal.pgen.1003016

Makarova, A. V., and P. M. Burgers, 2015 Eukaryotic DNA polymerase zeta. DNA Repair (Amst.) 29: 47–55. https://doi.org/10.1016/j.dnarep.2015.02.012

Malkova, A., and J. E. Haber, 2012 Mutations arising during repair of chromosome breaks. Annu. Rev. Genet. 46: 455–473. https://doi.org/10.1146/annurev-genet-110711-155547

Mann, H. B., and D. R. Whitney, 1947 On a test of whether one of two random variables is stochastically larger than the other. Ann. Math. Stat. 18: 50–60. https://doi.org/10.1214/aoms/1177730491

Marsischky, G. T., N. Filosi, M. F. Kane, and R. Kolodner, 1996 Redundancy of Saccharomyces cerevisiae MSH3 and MSH6 in MSH2-dependent mismatch repair. Genes Dev. 10: 407–420. https://doi.org/10.1101/gad.10.4.407

McVey, M., V. Y. Khodaverdian, D. Meyer, P. G. Cerqueira, and W.-D. Heyer, 2016 Eukaryotic DNA polymerases in homologous recombination. Annu. Rev. Genet. 50: 393–421. https://doi.org/10.1146/annurev-genet-120215-035243

Melixetian, M., A. Ballabeni, L. Masiero, P. Gasparini, R. Zamponi *et al.*, 2004 Loss of Geminin induces rereplication in the presence of functional p53. J. Cell Biol. 165: 473–482. https://doi.org/10.1083/jcb.200403106

Menghi, F., K. Inaki, X. Woo, P. A. Kumar, K. R. Grzeda *et al.*, 2016 The tandem duplicator phenotype as a distinct genomic configuration in cancer. Proc. Natl. Acad. Sci. USA 113: E2373–E2382. https://doi.org/10.1073/pnas.1520010113

Modrich, P., 2016 Mechanisms in E. coli and human mismatch repair (Nobel lecture). Angew. Chem. Int. Ed. Engl. 55: 8490–8501. https://doi.org/10.1002/anie.201601412

Morrison, A., and A. Sugino, 1994 The 3′→ 5′ exonucleases of both DNA polymerases delta and epsilon participate in correcting errors of DNA replication in Saccharomyces cerevisiae. Mol. Gen. Genet. 242: 289–296. https://doi.org/10.1007/BF00280418

Morrison, A., J. B. Bell, T. A. Kunkel, and A. Sugino, 1991 Eukaryotic DNA polymerase amino acid sequence required for 3′—-5′ exonuclease activity. Proc. Natl. Acad. Sci. USA 88: 9473–9477. https://doi.org/10.1073/pnas.88.21.9473

Morrison, A., A. L. Johnson, L. H. Johnston, and A. Sugino, 1993 Pathway correcting DNA replication errors in Saccharomyces cerevisiae. EMBO J. 12: 1467–1473. https://doi.org/10.1002/j.1460-2075.1993.tb05790.x

Nguyen, V. Q., C. Co, K. Irie, and J. J. Li, 2000 Clb/Cdc28 kinases promote nuclear export of the replication initiator proteins Mcm2–7. Curr. Biol. 10: 195–205. https://doi.org/10.1016/S0960-9822(00)00337-7

Nguyen, V. Q., C. Co, and J. J. Li, 2001 Cyclin-dependent kinases prevent DNA re-replication through multiple mechanisms. Nature 411: 1068–1073. https://doi.org/10.1038/35082600

Northam, M. R., E. A. Moore, T. M. Mertz, S. K. Binz, C. M. Stith *et al.*, 2014 DNA polymerases ζ and Rev1 mediate error-prone

bypass of non-B DNA structures. Nucleic Acids Res. 42: 290–306. https://doi.org/10.1093/nar/gkt830

Pavlov, Y. I., C. Frahm, S. A. Nick McElhinny, A. Niimi, M. Suzuki *et al.*, 2006 Evidence that errors made by DNA polymerase α are corrected by DNA polymerase δ. Curr. Biol. 16: 202–207. https://doi.org/10.1016/j.cub.2005.12.002

Peltomäki, P., 2016 Update on Lynch syndrome genomics. Fam. Cancer 15: 385–393. https://doi.org/10.1007/s10689-016-9882-8

Perkins, G., L. S. Drury, and J. F. Diffley, 2001 Separate SCF(CDC4) recognition elements target Cdc6 for proteolysis in S phase and mitosis. EMBO J. 20: 4836–4845. https://doi.org/10.1093/emboj/20.17.4836

Pluciennik, A., L. Dzantiev, R. R. Iyer, N. Constantin, F. A. Kadyrov *et al.*, 2010 PCNA function in the activation and strand direction of MutLα endonuclease in mismatch repair. Proc. Natl. Acad. Sci. USA 107: 16066–16071. https://doi.org/10.1073/pnas.1010662107

Richardson, C. D., and J. J. Li, 2014 Regulatory mechanisms that prevent re-initiation of DNA replication can be locally modulated at origins by nearby sequence elements. PLoS Genet. 10: e1004358. https://doi.org/10.1371/journal.pgen.1004358

Schmidt, T. T., G. Reyes, K. Gries, C. U. Ceylan, S. Sharma *et al.*, 2017 Alterations in cellular metabolism triggered by URA7 or GLN3 inactivation cause imbalanced dNTP pools and increased mutagenesis. Proc. Natl. Acad. Sci. USA 114: E4442–E4451. https://doi.org/10.1073/pnas.1618714114

Seo, J., Y. S. Chung, G. G. Sharma, E. Moon, W. R. Burack *et al.*, 2005 Cdt1 transgenic mice develop lymphoblastic lymphoma in the absence of p53. Oncogene 24: 8176–8186. https://doi.org/10.1038/sj.onc.1208881

Shcherbakova, P. V., and T. A. Kunkel, 1999 Mutator phenotypes conferred by MLH1 overexpression and by heterozygosity for mlh1 mutations. Mol. Cell. Biol. 19: 3177–3183. https://doi.org/10.1128/MCB.19.4.3177

Siddiqui, K., K. F. On, and J. F. Diffley, 2013 Regulating DNA replication in eukarya. Cold Spring Harb. Perspect. Biol. 5: a012930. https://doi.org/10.1101/cshperspect.a012930

Sikorski, R. S., and P. Hieter, 1989 A system of shuttle vectors and yeast host strains designed for efficient manipulation of DNA in Saccharomyces cerevisiae. Genetics 122: 19–27.

St Charles, J. A., S. E. Liberti, J. S. Williams, S. A. Lujan, and T. A. Kunkel, 2015 Quantifying the contributions of base selectivity, proofreading and mismatch repair to nuclear DNA replication in Saccharomyces cerevisiae. DNA Repair (Amst.) 31: 41–51. https://doi.org/10.1016/j.dnarep.2015.04.006

Strathern, J. N., B. K. Shafer, and C. B. McGill, 1995 DNA synthesis errors associated with double-strand-break repair. Genetics 140: 965–972.

Tatsumi, Y., N. Sugimoto, T. Yugawa, M. Narisawa-Saito, T. Kiyono *et al.*, 2006 Deregulation of Cdt1 induces chromosomal damage without rereplication and leads to chromosomal instability. J. Cell Sci. 119: 3128–3140. https://doi.org/10.1242/jcs.03031

Tran, H. T., J. D. Keen, M. Kricker, M. A. Resnick, and D. A. Gordenin, 1997 Hypermutability of homonucleotide runs in mismatch repair and DNA polymerase proofreading yeast mutants. Mol. Cell. Biol. 17: 2859–2865. https://doi.org/10.1128/MCB.17.5.2859

Tran, H. T., D. A. Gordenin, and M. A. Resnick, 1999 The 3′→5′ exonucleases of DNA polymerases delta and epsilon and the 5′→3′ exonuclease exo1 have major roles in postreplication mutation avoidance in Saccharomyces cerevisiae. Mol. Cell. Biol. 19: 2000–2007. https://doi.org/10.1128/MCB.19.3.2000

Truong, L. N., and X. Wu, 2011 Prevention of DNA re-replication in eukaryotic cells. J. Mol. Cell Biol. 3: 13–22. https://doi.org/10.1093/jmcb/mjq052

Vaisman, A., and R. Woodgate, 2017 Translesion DNA polymerases in eukaryotes: what makes them tick? Crit. Rev. Biochem. Mol. Biol. 52: 274–303. https://doi.org/10.1080/10409238.2017.1291576

Vaziri, C., S. Saxena, Y. Jeon, C. Lee, K. Murata *et al.*, 2003 A p53-dependent checkpoint pathway prevents rereplication. Mol. Cell 11: 997–1008. https://doi.org/10.1016/S1097-2765(03)00099-6

Vogelstein, B., and K. W. Kinzler, 2004 Cancer genes and the pathways they control. Nat. Med. 10: 789–799. https://doi.org/10.1038/nm1087

Wielders, E. A., J. Hettinger, R. Dekker, C. M. Kets, M. J. Ligtenberg *et al.*, 2014 Functional analysis of MSH2 unclassified variants found in suspected Lynch syndrome patients reveals pathogenicity due to attenuated mismatch repair. J. Med. Genet. 51: 245–253. https://doi.org/10.1136/jmedgenet-2013-101987

Zhao, G., Y. Chen, L. Carey, and B. Futcher, 2016 Cyclin-dependent kinase co-ordinates carbohydrate metabolism and cell cycle in S. cerevisiae. Mol. Cell 62: 546–557. https://doi.org/10.1016/j.molcel.2016.04.026

Zhu, W., Y. Chen, and A. Dutta, 2004 Rereplication by depletion of geminin is seen regardless of p53 status and activates a G2/M checkpoint. Mol. Cell. Biol. 24: 7140–7150. https://doi.org/10.1128/MCB.24.16.7140-7150.2004

Communicating editor: B. Calvi